



Transport and mixing in the TTL

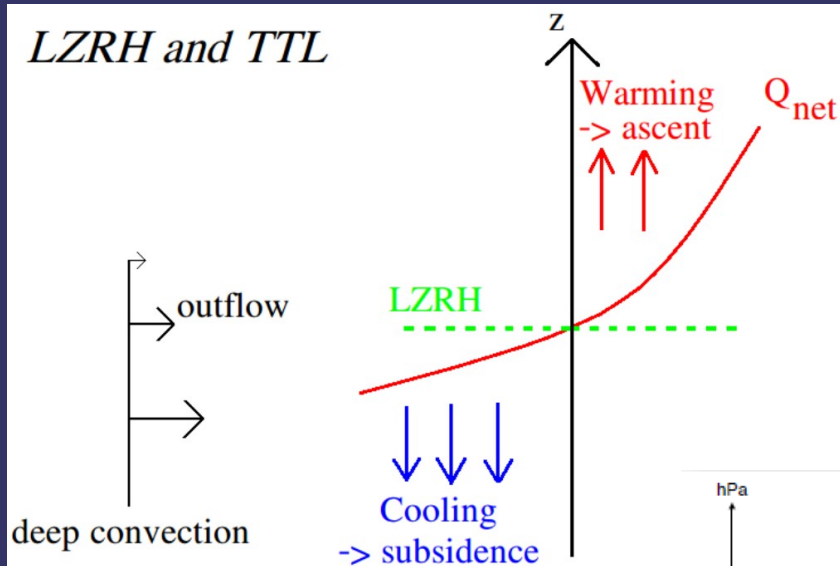
Convective sources

Bernard Legras, Ann'Sophie Tissier

Laboratoire de Météorologie Dynamique, IPSL, CNRS/UPMC/ENS, France

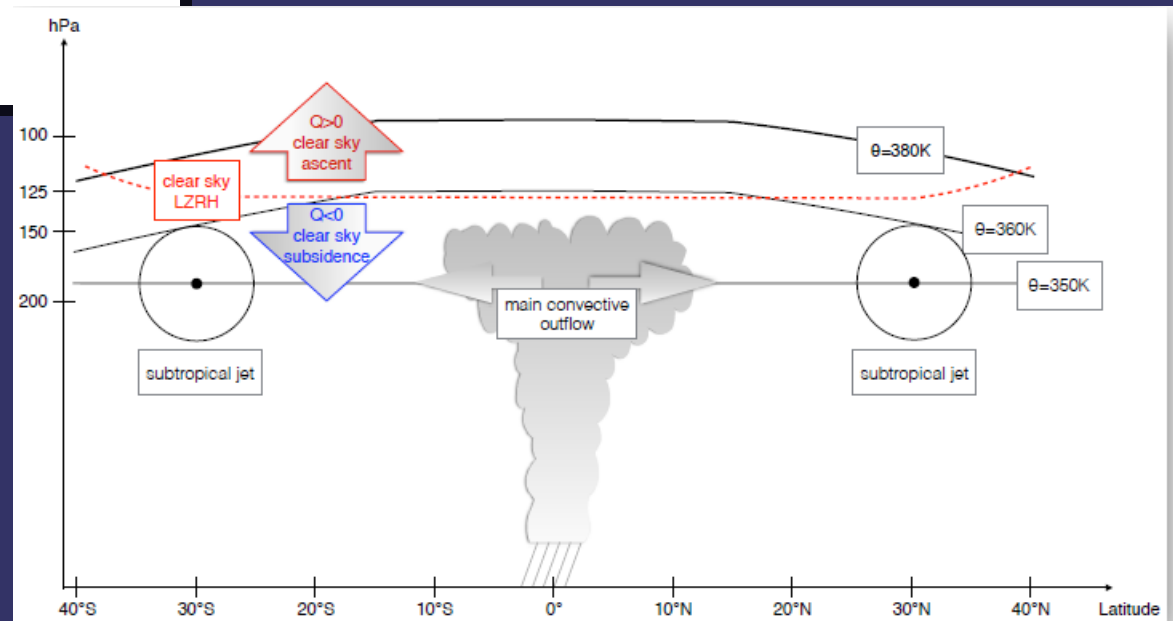
Based on Tissier & Legras, ACPD, 2015

Transition of radiative heating in the TTL from negative to positive values



Schematic of troposphere-to-stratosphere transport pathway.

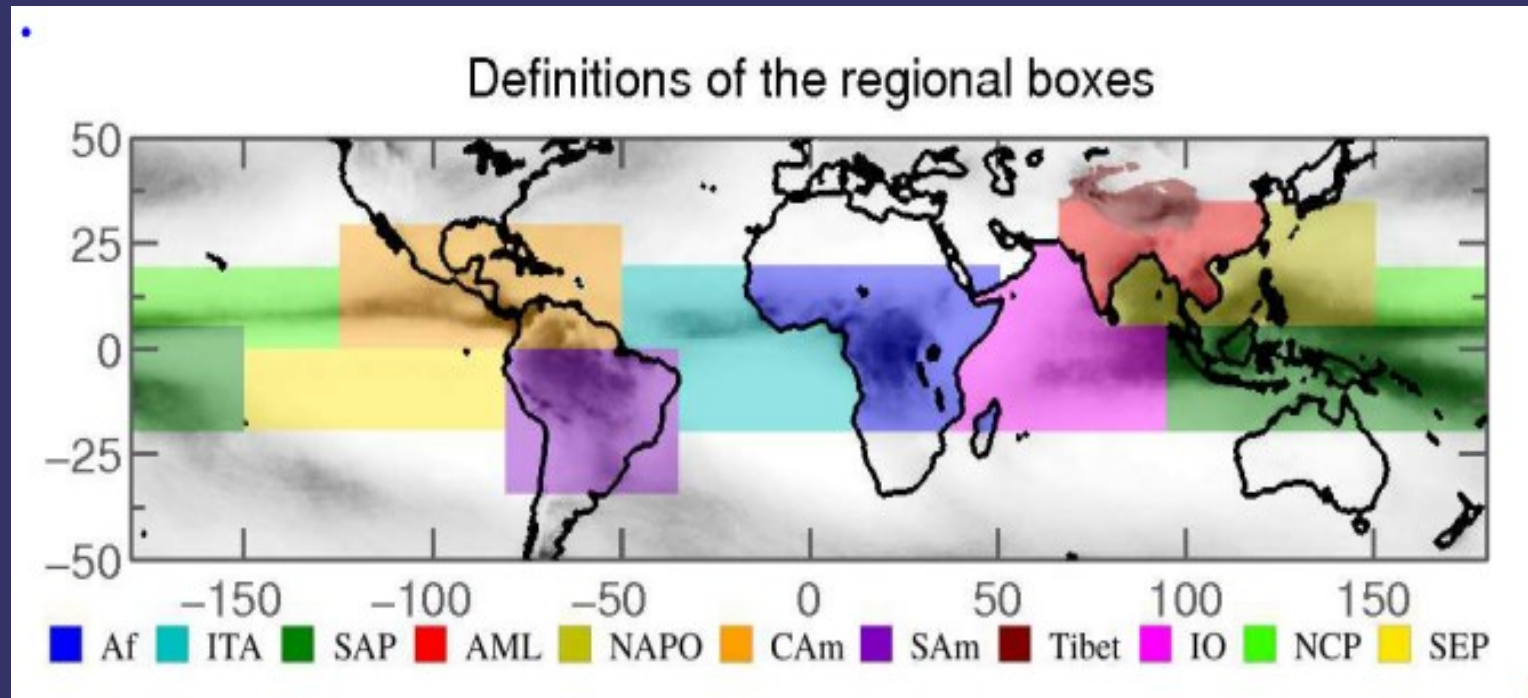
The Level of Zero Radiative Heating (LZRH) is above the mean level of convective outflow. It divides ascending (above) and descending (below) motion.
(Corti et al., 2006)



General questions

- How parcels detrained by convection are transported in the TTL, across the level of zero heating ?
- What is the horizontal and vertical distribution of the convective sources ?
- What is the residence time of parcels within the TTL ?
- Seasonal and regional variability?

Regional boxes are defined over the major contributing sources, separating continental from maritime convection



Af : Africa

ITA : Inter Tropical Atlantic

SAP ; South Asia – Pacific

AML : Asia Main Land

NAPO : North Asia – Pacific / Ocean

Cam : Central America

Sam : South America

Tibet : Tibetan plateau (orography > 3800m)

IO : Indian Ocean

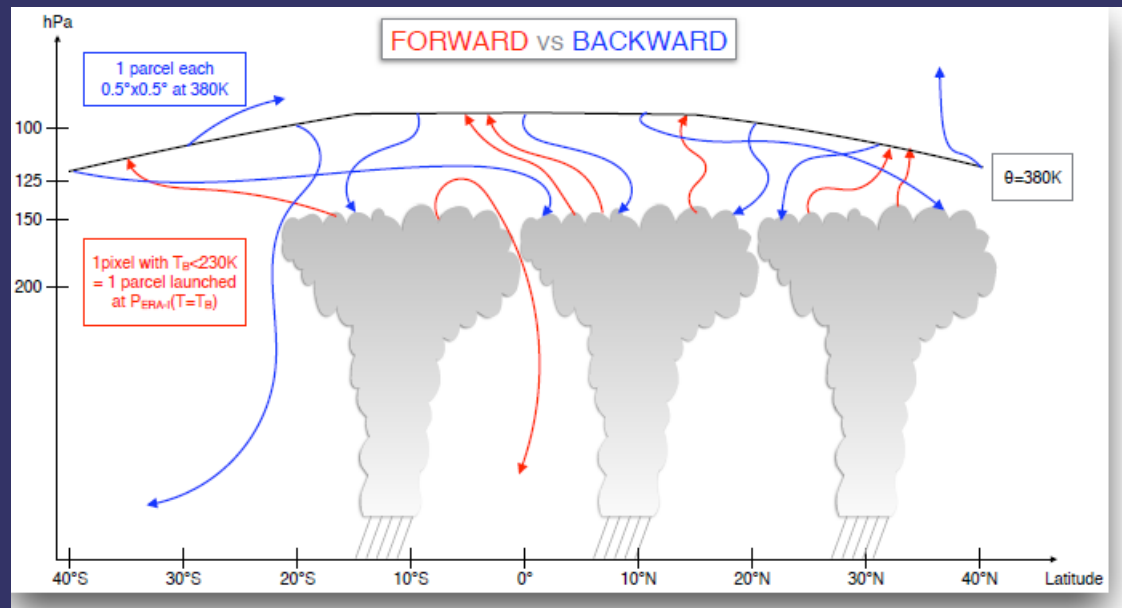
NCP/ North Central Pacific

SEP : South East Pacific

Trajectory calculations with TRACZILLA

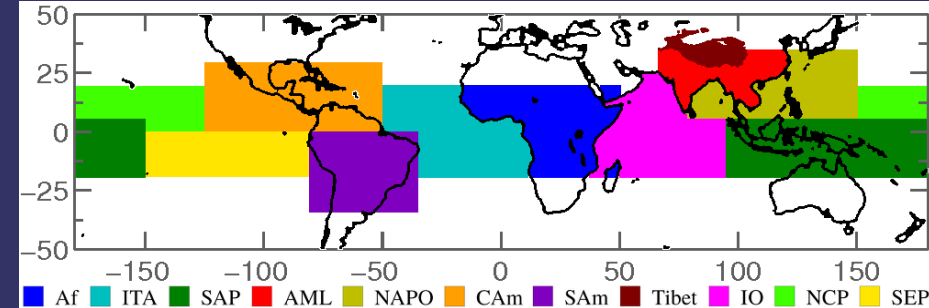
- TRACZILLA : modified version of FLEXPART ([Stohl and al, 2005], [Pisso and Legras, 2008])
- Calculations of **forward diabatic** and **backward diabatic** trajectories.
- Trajectories are updated every 15 minutes.
- Horizontal part of the movement : calculated using **wind fields of ERA-Interim**.
- Vertical part of the movement : calculated using **radiative heating rates of ERA-Interim**.
- No latent heat.

Diabatic trajectories :
Horizontal motion due to horizontal wind
Vertical displacement by heating rates using potential temperature θ as coordinate.
3-hourly data for ERA-Interim, 6-hourly for JRA-55
Reference surface $\theta=380\text{K}$
3-month trajectories



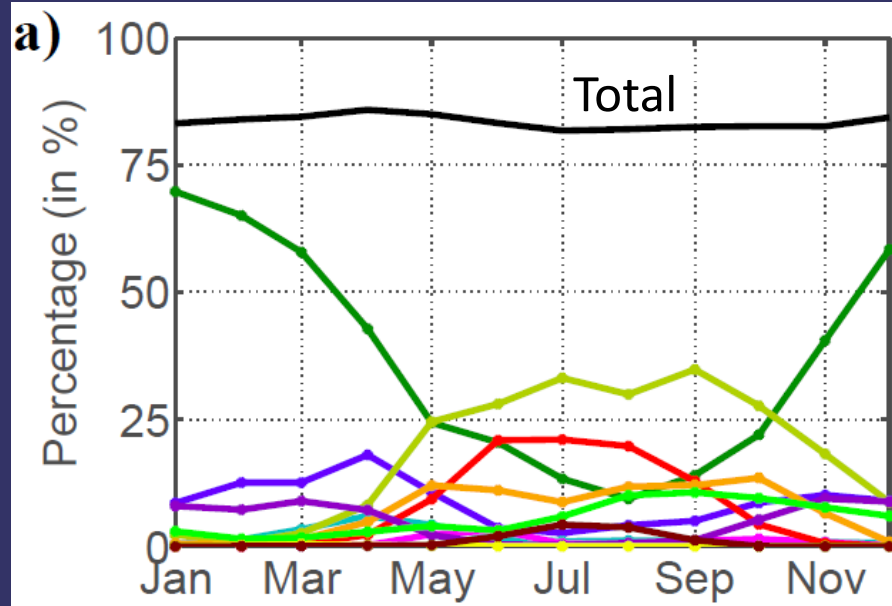
Backward launching : 1 parcel on $0.5^\circ \times 0.5^\circ$ grid on 40S-40N every two days, stopped at first encounter of cloud top + 1km
Forward launching : 1 parcel at cloud top + 1km for each CLAUS pixel (3h and 30km resolution) at $T < 230\text{K}$, stopped at first encounter of 380K surface

Source distribution among regions (2005-2008 ERA-Interim)



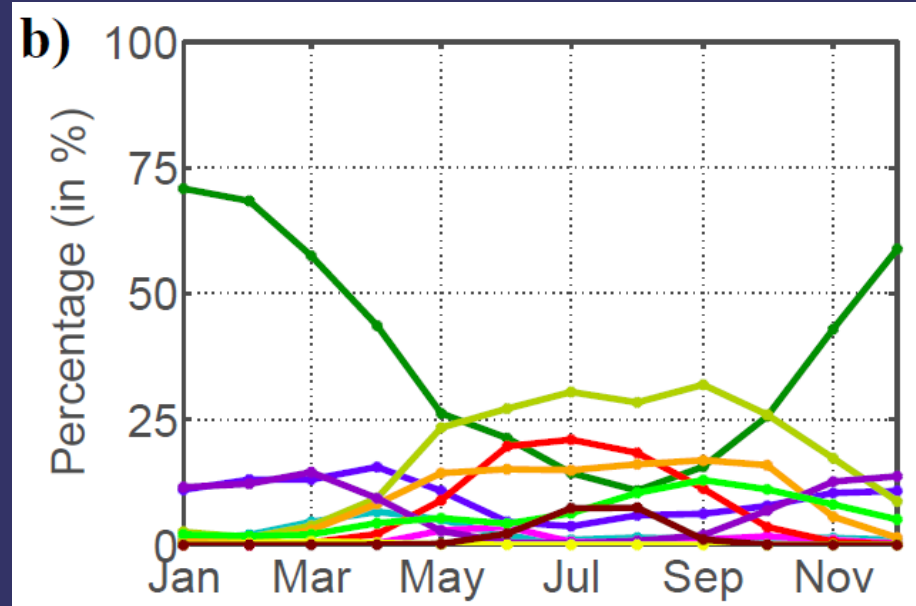
Backward

Forward



of parcels which have reached the top of a cloud in the region

Total # of parcels which have reached the top of a cloud



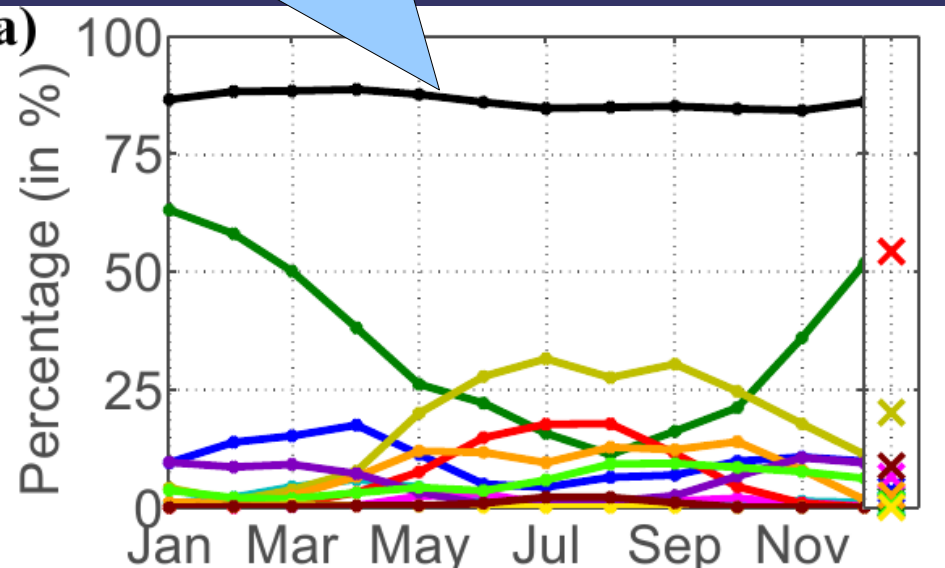
of parcels which have reached 380K from a given region

Total # of parcels which have reached 380K from all regions

Domination of SAP during winter and of Asian sources (NAPO+AML) and Central America (CAm) during summer. Notice the African peak in April. Excellent agreement between backward and forward indicates statistical robustness.

2005-2008 ERA-Interim

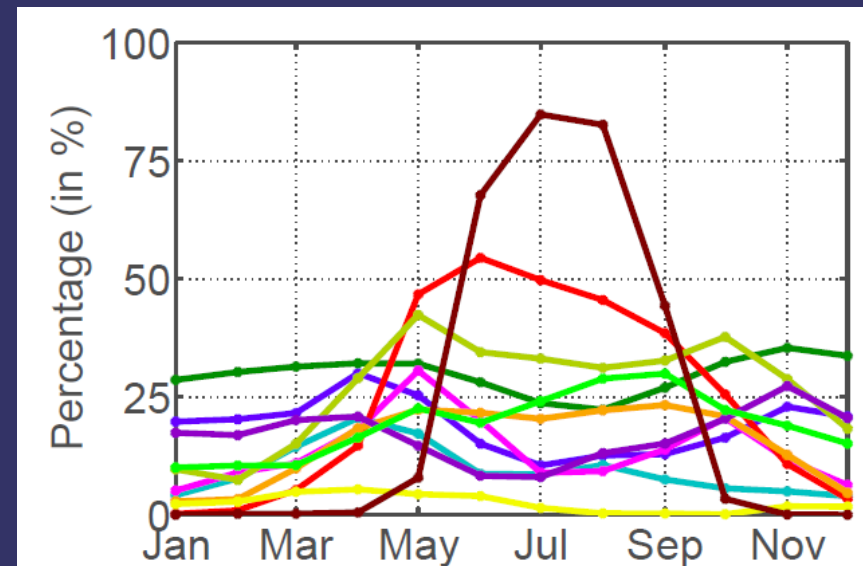
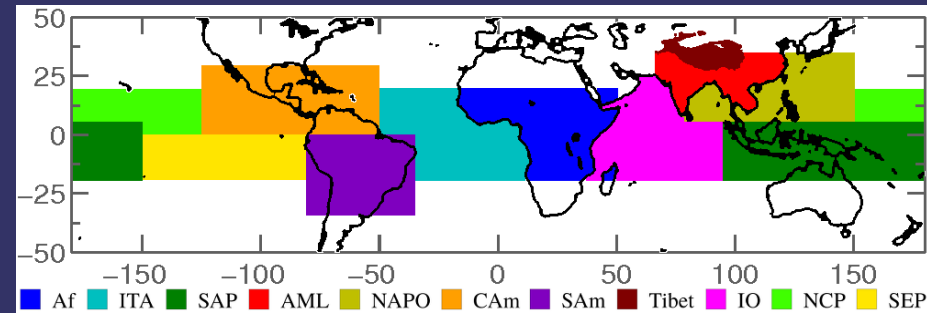
Proportion of parcels launched at 380K, reaching a cloud within 3 months ~ 82 %



of parcels which have reached
the top of a cloud in the box

Total # of parcels which have reached
the top of a cloud

Weight of the source regions



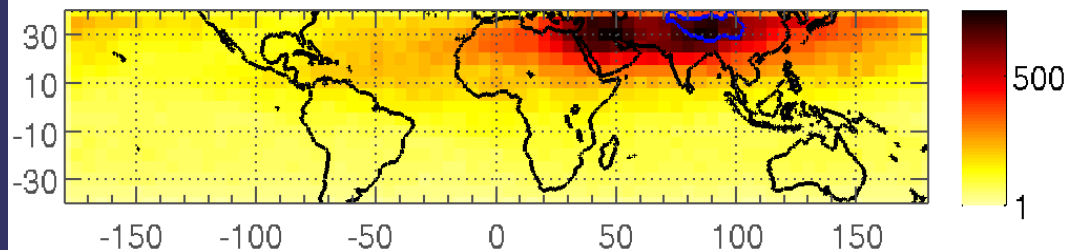
of parcels which have reached 380K
of parcels launched from the box

Efficiency of the source regions

During summer, the Tibetan plateau, in spite of its small total contribution, is the most efficient region in transporting air parcels from cloud top to 380K.

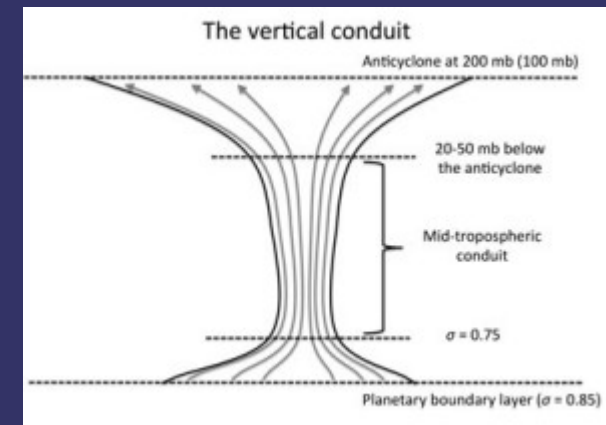
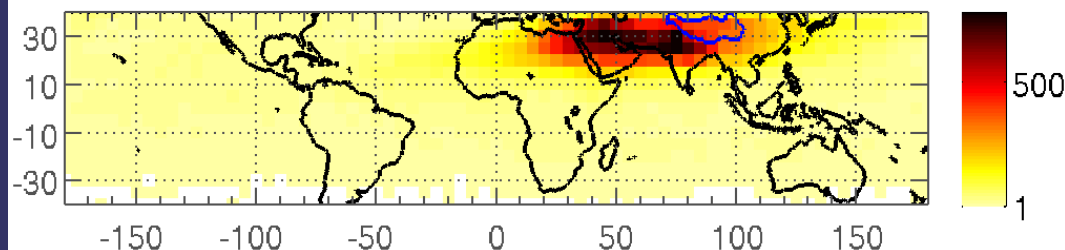
Backward

Position of the Tibet2 parcels at 380K : JJA



Forward

Position of the Tibet2 parcels at 380K : JJA



Bergman et al.,
ACP 2013

Distribution of the upward flux
among the source regions and
over the months.

2005-2008 average for ERA-
Interim

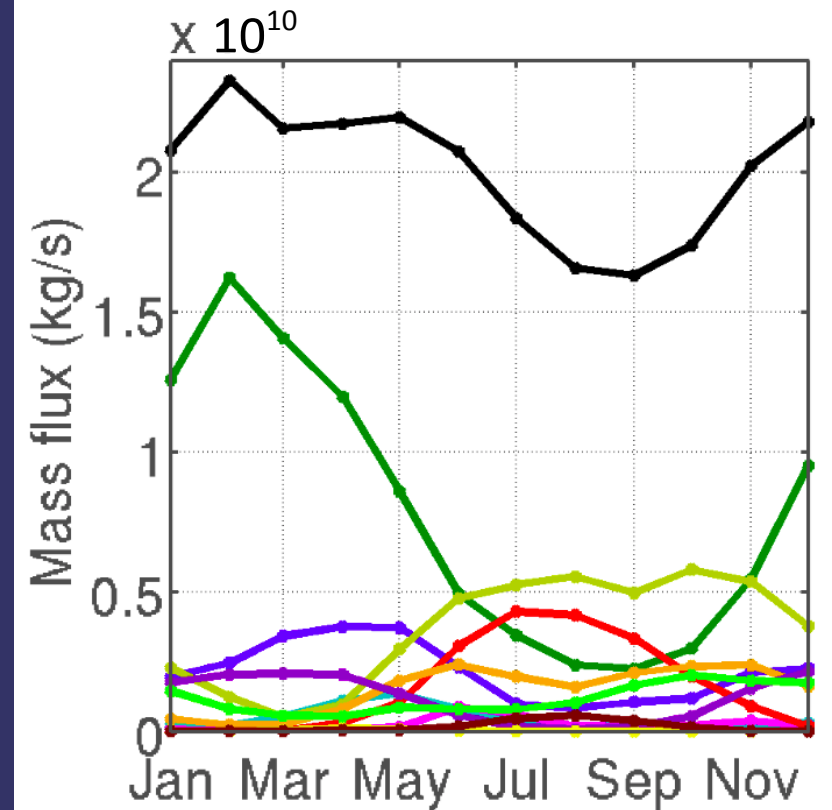
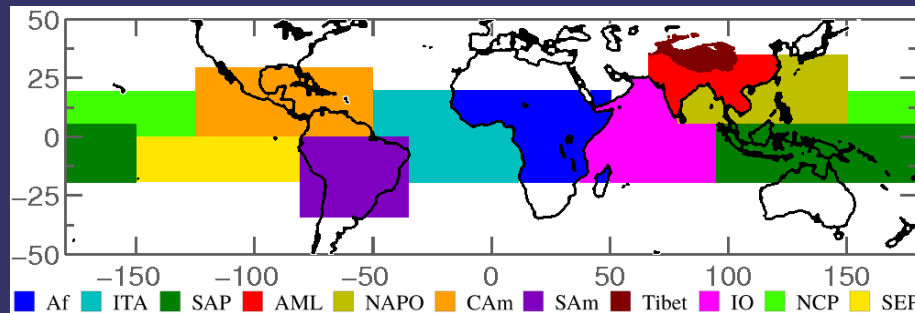


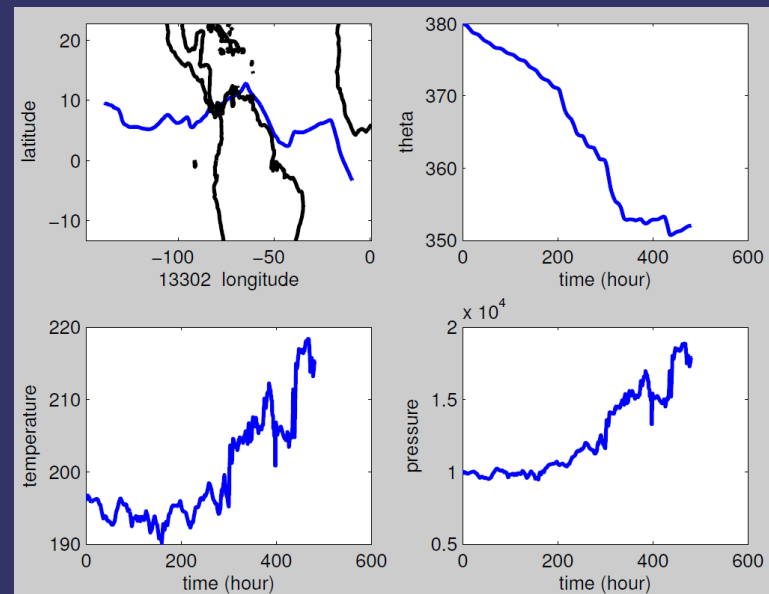
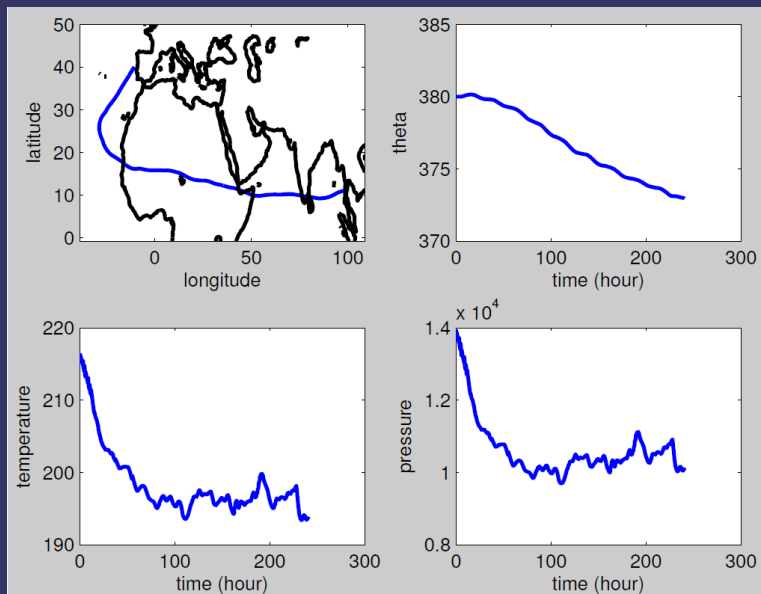
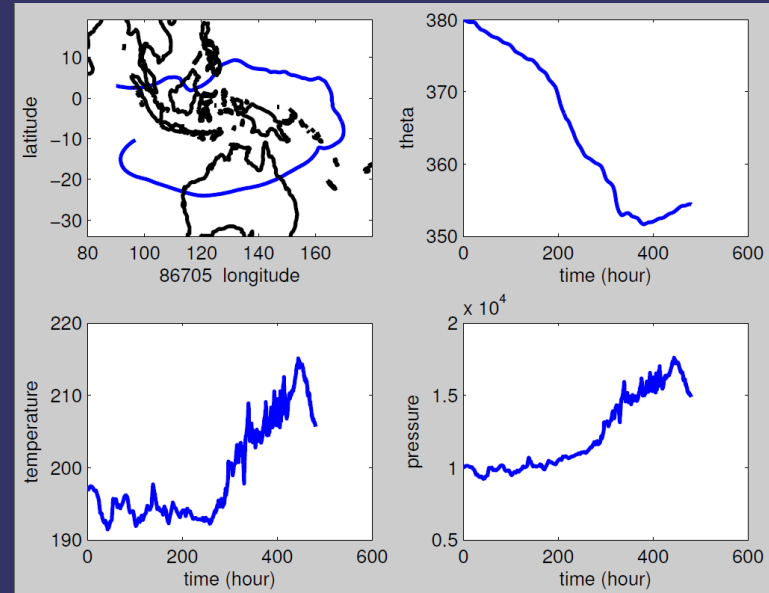
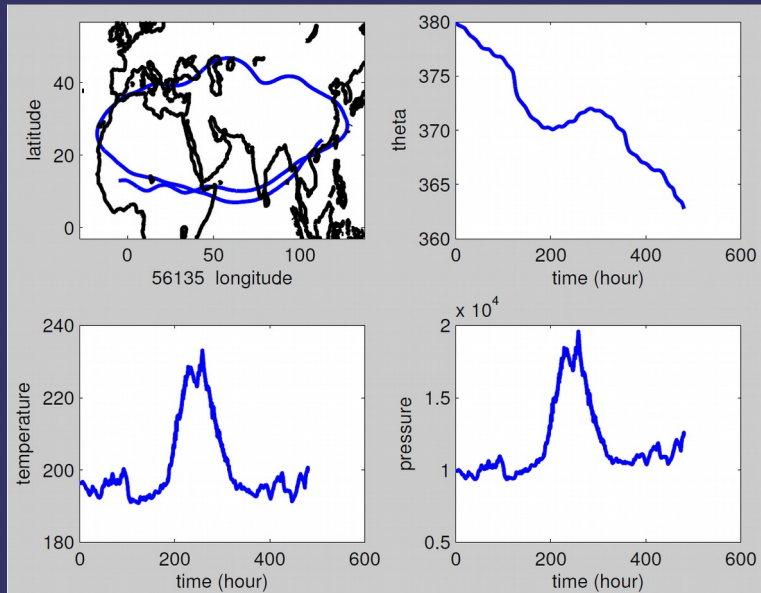
Table 4. Distribution of annual mass flux, averaged over 2005–2008, for all the regions (in %).

Af	ITA	SAP	AML	NAPO	CAM	SAM	Tibet	IO	NCP	SEP
10.8	2.4	39.2	8	18	7.5	6	0.8	1.2	5.9	0.2

The mass flux inherits the properties of the source distribution with slight modifications (SAP flux still larger than CAM flux during summer) .

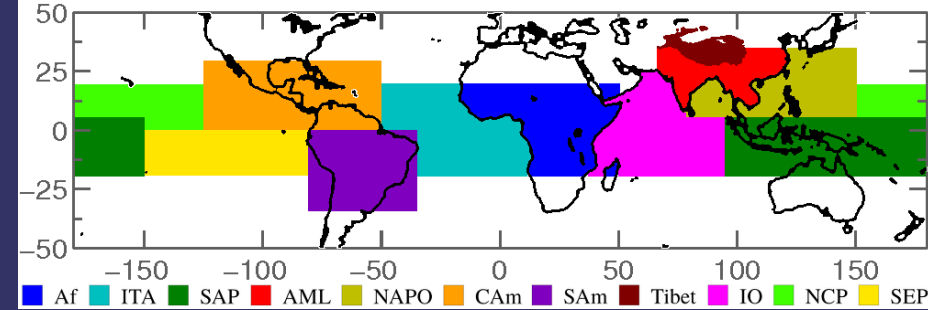
CAUTION : This is not the mass flux of convective air across 380K surface as it does not account for mixing of detrained air with the environment at the top of clouds.

Examples of backward trajectories

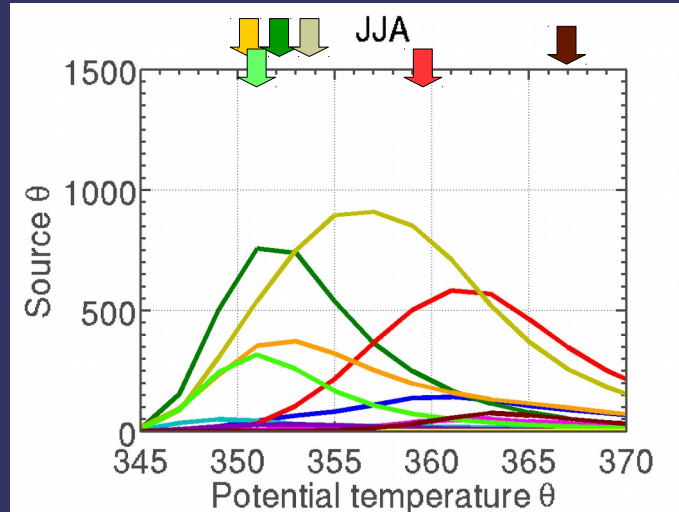
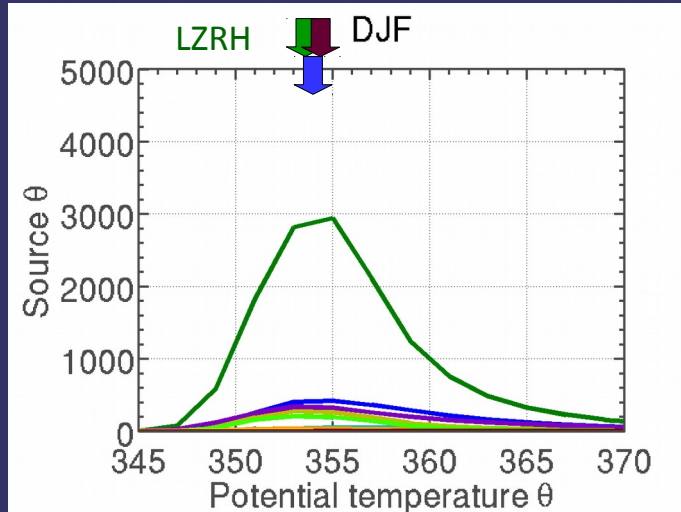


Vertical distribution of sources (2005-2008 ERA-Interim)

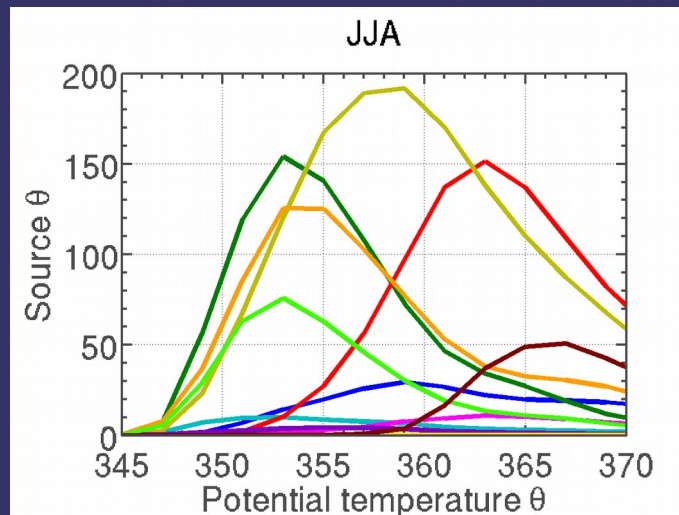
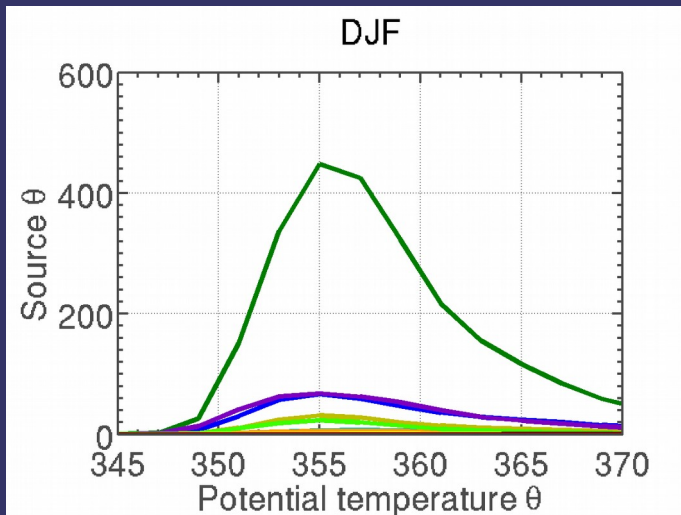
Asian monsoon sources, especially continental, at higher levels than Pacific maritime sources and above all sky LZRH (but for Tibet).



Backward

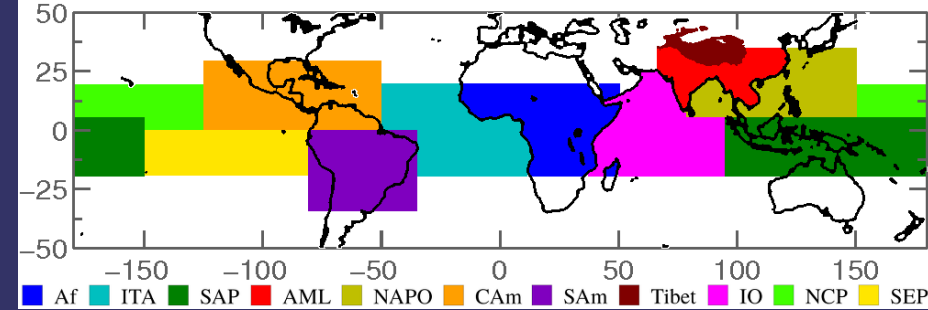


Forward

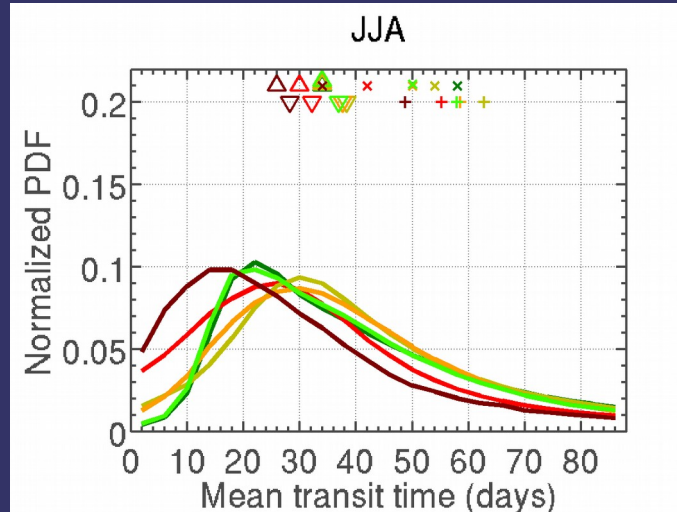
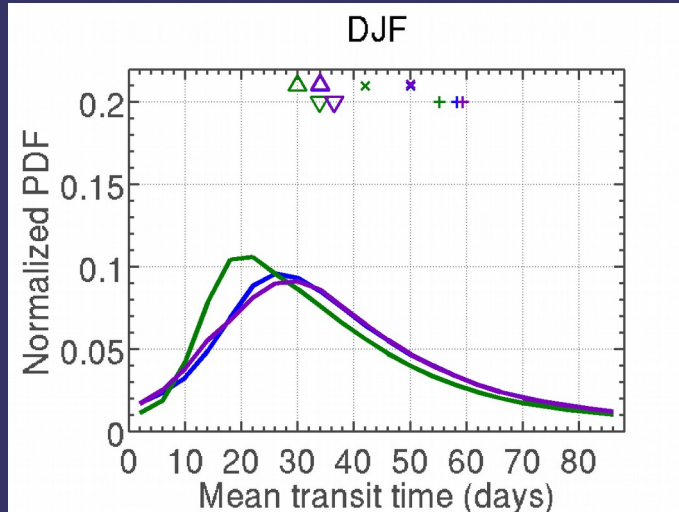


Distribution of transit times (2005-2008 ERA-Interim)

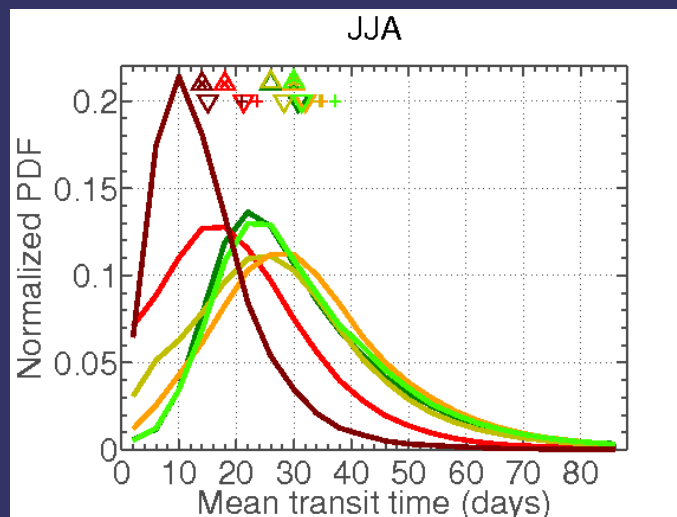
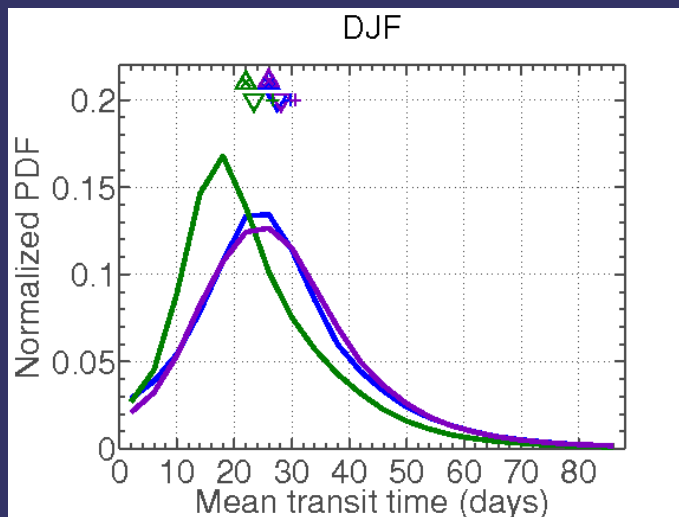
Backward transit times are shifted to large values with respect to forward times due to the intermittency of cloud encounter and recirculations, especially over Asia.



Backward



Forward



Conclusion

Reproducible results by both forward and backward calculations show that even a fairly rough sampling (50 km/2 days in backward, one parcel per high 30kmx30kmX3h pixel in forward) provides cloud to 380K transport statistics for most regions.

The sources are vertically distribute in the vicinity of the all sky level of zero radiative heating but mostly above (75-80%) except for Tibet (50%) , that is well above the mean level of convective outflow. The LZRH and sources are higher over continental convection.

The South Asia Pacific region (warmpool) is the main contributor during winter season (actually half of the year) while Asian Land and Asian Ocean regions are the largest contributors during summer and the Asian monsoon.

Trapping within the Asian Monsoon Anticyclone is most effective for parcels released by convection over the Tibetan plateau but the Tibetan plateau remains an overall small contributor to transport of convective air to the stratosphere.

The mass flux across the 380K surface that originates from the region of convective outflow can be estimated .

Among modern reanalysis, ERA-Interim and JRA-55 show qualitatively similar results but also some differences (higher sources and shorter transfer times in JRA-55) .

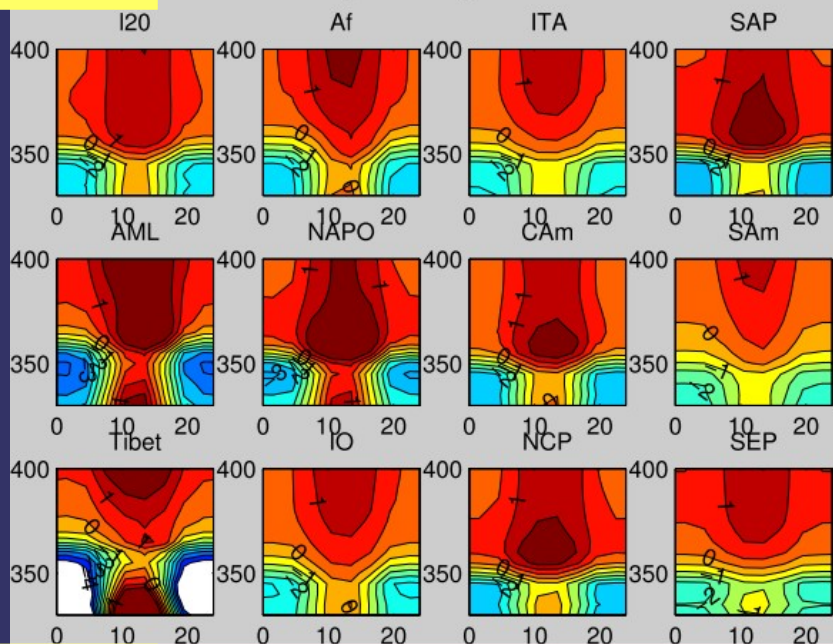
Questions

What is the uncertainty induced by differences between the re-analysis ? Which heating rates are the most reliable ? Unresolved motion and LZRH crossing?

How to estimate the flux of air across the 380K surface that has been recently processed by convection ? In other words, how to estimate detrainment and mixing at and above the level of convective outflow ?

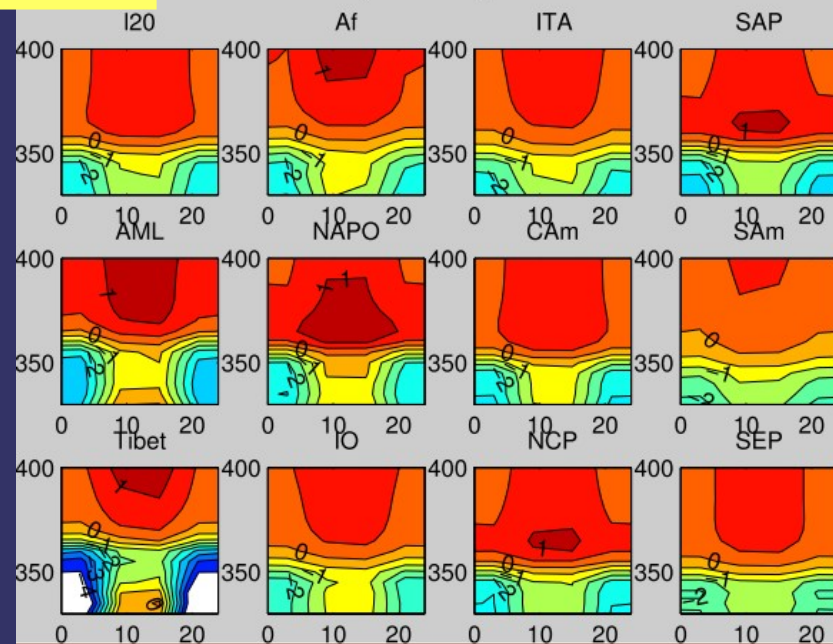
ECMWF

ERA-I Daily ashr cycle :Jul-2005



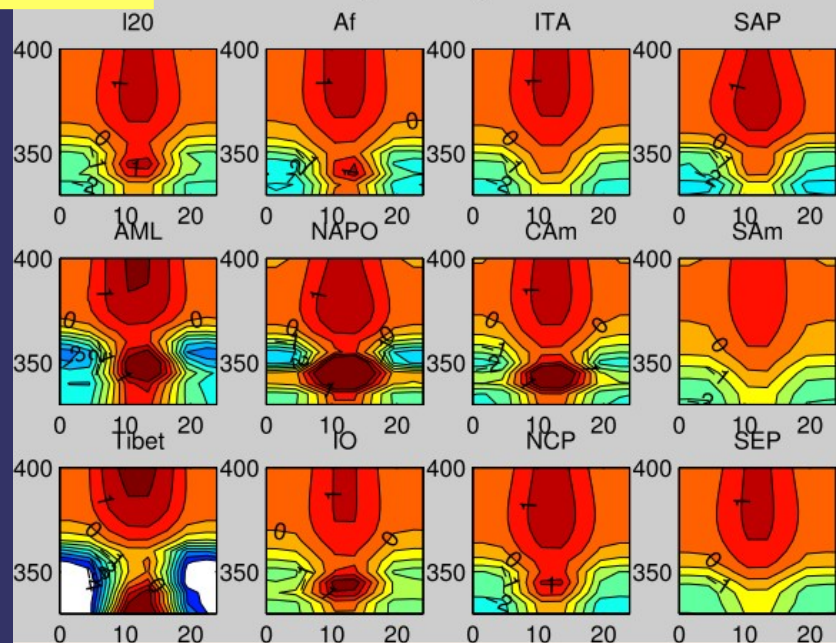
JMA

JRA-55 Daily ashr cycle :Jul-2005



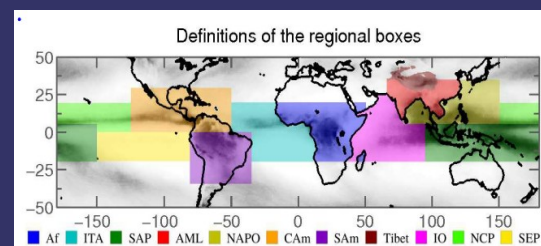
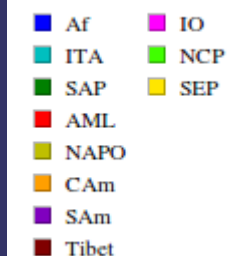
NASA

MERRA Daily ashr cycle :Jul-2005



All sky heating rate
cycle (averaged in
local time)

July 2005



Caveats and questions to be addressed within Stratoclim

The distribution of sources and transit times are sensitive to the representation of cloud tops.

There are also differences between reanalysis due to their differences in heating rates.

There are differences with other studies :

- with Heath & Fuelberg 2014) : they find more than 80 % of AMA air from continental Asia as us but more weight to the Tibetan plateau.
- with Chen et al., 2012 : transit times from the PBL to the stratosphere with a peak at 3 days
- with Orbe et al., 2015 : two month transit time from the PBL

What is the uncertainty induced by differences between the re-analysis ? Which heating rates are the most reliable ?

What is the effect of unresolved motion ?

How to estimate the flux of air across the 380K surface that has been recently processed by convection ? In other words, how to estimate detrainment and mixing at and above the level of convective outflow ?

Can we refine the distribution of sources with a more detailed description of regions ?

What is the impact of using high resolution cloud tops and cloud classifications ?

What is the impact of convection overshooting the anvil ?